SCIENCE CHINA
Chemistry

• ARTICLES •

April 2013 Vol.56 No.4: 505–513
doi: 10.1007/s11426-012-4758-8

D-A-π-A organic sensitizers containing a benzothiazole moiety as an additional acceptor for use in solar cells

ZENG Juan[1], ZHANG TengLong[2], ZANG XuFeng[1], KUANG DaiBin[2*], MEIER Herbert[3] & CAO DeRong[1*]

[1]*School of Chemistry and Chemical Engineering, State Key Laboratory of Luminescent Materials and Devices, South China University of Technology, Guangzhou 510641, China*

[2]*MOE Key Laboratory of Bioinorganic and Synthetic Chemistry, KLGHEI of Environment and Energy Chemistry, School of Chemistry and Chemical Engineering, Sun Yat-sen University, Guangzhou 510275, China*

[3]*Institute of Organic Chemistry, University of Mainz, Mainz 55099, Germany*

Received July 15, 2012; accepted August 20, 2012; published online September 15, 2012

Three novel triphenylamine-based D-A-π-A-featured dyes (**Z1–Z3**) have been designed, synthesized and characterized for use in dye-sensitized solar cells. Benzothiazole was incorporated as an additional acceptor, which greatly enhanced the molar extinction coefficient of the dyes. Various conjugated linkers, such as benzene, furan and thiophene, were also introduced to configure the novel D-A-π-A framework in order to prolong electron flow and active transportation. Among all dyes, **Z2** containing a thiophene linker exhibited the maximum overall conversion efficiency (η) of 4.16% (J_{sc} = 9.27 mA cm^{-2}, V_{oc} = 642 mV, FF = 0.70) under standard global AM 1.5 G solar condition.

organic dye, dye-sensitized solar cell, D-A-π-A, benzothiazole

1 Introduction

Solar energy is considered to be the most important renewable energy resource in the 21st century. As a new generation of photovoltaic devices, dye-sensitized solar cells (DSSCs) have drawn immense attention since the initial reports by Grätzel and co-workers [1–5] because of their high efficiency, low cost, and facile fabrication. In DSSCs, the sensitizer can be an organic ligand-metal complex or a metal-free organic dye, and is one of the key components for high power conversion efficiency. Nowadays, some DSSCs based on Ru complexes have achieved remarkable power conversion efficiencies of more than 11% [6–8]. However, metal-free organic dyes have recently emerged as an alternative to Ru dyes owing to their high molar absorption coefficients, simple syntheses, low costs, and easy structural modifications [9]. A variety of organic dyes such as coumarin [10, 11], merocyanine [12], indoline [13–15], hemicyanine [16, 17], triphenylamine [18–25], and phenothiazine [26–29] have been investigated for DSSCs and show good performances.

The chemical structures of metal-free organic dyes are crucial for high power-conversion efficiency. Many researchers have devoted themselves to optimize chemical structures for improvements in performance. Recently, Tian *et al*. [30–32] reported a series of novel donor-acceptor-π-bridge-acceptor (D-A-π-A) organic dyes incorporating an additional acceptor such as benzothiadiazole, benzotriazole and quinoxaline into the traditional D-π-A framework. The additional acceptor chromophore is expected to facilitate the electron transfer from the donor to the acceptor, and has diverse effects on the photovoltaic performances in the D-A-π-A configuration [32]. Thus it is important to find

*Corresponding authors (email: kuangdb@mail.sysu.edu.cn; drcao@scut.edu.cn)

new and appropriate additional acceptors in the D-A-π-A framework.

Benzothiazole is a well-known electron-withdrawing unit, and has the characteristics of high chemical and photophysical stability. It has been widely investigated in the construction of dyes with enhanced two photon absorption [33, 34]. To the best of our knowledge, the application of benzothiazole acceptors in D-A-π-A systems has never been reported before. Here we introduce the benzothiazole unit into triphenylamine-based dyes to develop a series of novel D-A-π-A sensitizers (Scheme 1). The photophysical properties, electrochemical properties and photovoltaic performance of this D-A-π-A system have been investigated in detail.

2 Experimental

2.1 Instrumentation and materials

NMR (^{1}H and ^{13}C) spectra were recorded on a Bruker 400 MHz spectrometer (in $CDCl_3$ or DMSO-d_6, TMS as the internal reference). Mass spectra were recorded on an Esquire HCT PLUS mass spectrometer. Elementary analyses were performed using a Vario EL III Analyzer. The melting points were measured on Tektronix X4 microscopic melting point apparatus and were uncorrected. The absorption and emission spectra were obtained in CH_2Cl_2 by using a Shimadzu UV-2450 spectrophotometer and a Fluorolog III photoluminescence spectrometer, respectively. Cyclic voltammetry measurements were carried out on an electrochemistry workstation (e-corder (ED 401) potentiostat) using a three-electrode cell. A TiO_2 film coated with the dye was used as a working electrode, with an Ag/AgCl (saturated KCl) reference electrode and a Pt counter electrode and a scan rate of 50 mV/s. Tetrabutylammonium perchlorate ($TBAPF_6$, 0.1 M) in acetonitrile was used as the supporting electrolyte. The measurements were calibrated using ferrocene (Fc) as a standard, and the potentials of dyes versus the normal hydrogen electrode (NHE) were calibrated by addition of 0.63 V to the potentials versus Fc^+/Fc. Current-

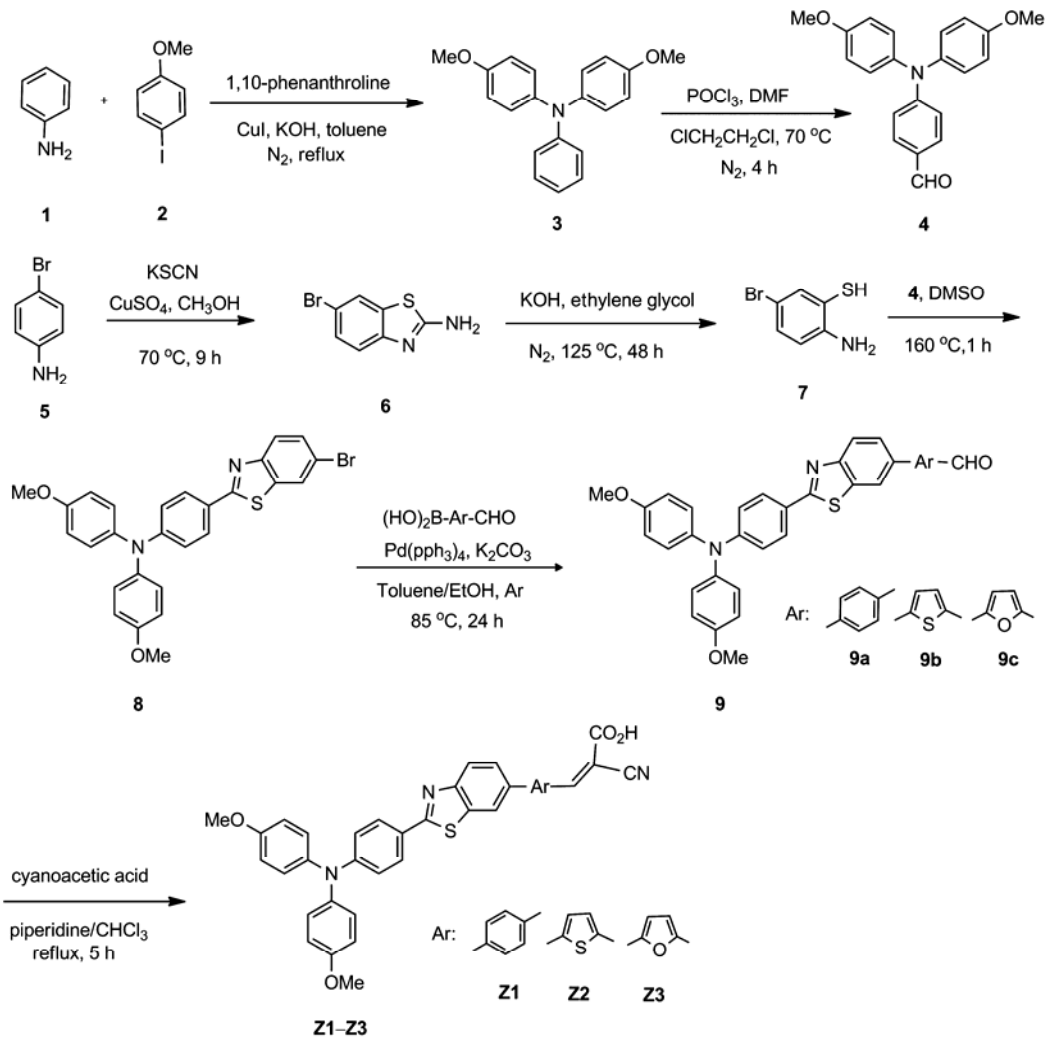

Scheme 1 Synthesis of dyes **Z1–Z3**.

voltage characteristics were performed on a Keithley 2400 source meter under simulated AM 1.5 G illumination (100 mW cm^{-2}) provided by a solar simulator (Oriel, Model 91192). A 1 kW Xe (Oriel, Model 6271) lamp with optical filter was used as light source. Incident photon-to-current conversion efficiency (IPCEs) spectra were taken on a Spectral Products DK240 monochromator as a function of wavelength from 350 to 800 nm. Electrochemical impedance spectroscopy (EIS) measurements were performed on a Zahner Zennium electrochemical workstation in the frequency range from 10 MHz to 1 mHz under dark conditions. The impedance parameters were determined by fitting of the impedance spectra using Z-view software. Intensity-modulated photovoltage spectroscopy (IMVS) was carried out on the electrochemical workstation (Zahner Zennium) with a frequency response analyzer under a modulated light emitting diode (457 nm) driven by a source supply (Zahner PP211). The light intensity modulation was 10% of the base light intensity over the frequency range from 100 kHz to 0.1 Hz.

Toluene and ethanol were dried and distilled from sodium under a nitrogen atmosphere. The boiling range of petroleum was 60–90 °C. All other solvents and reagents were obtained from commercially available resources without further purification.

2.2 Synthesis

*Bis-(4-methoxyphenyl)phenylamine (**3**)*

A mixture of aniline (2.28 mL, 25 mmol), 1-iodo-4-methoxybenzene (13.46 g, 57.50 mmol), KOH (11.60 g, 85%, 175.73 mmol), 1,10-phenanthroline (0.91 g, 4.60 mmol) and CuI (0.88 g, 4.60 mmol) in toluene (50 mL) was heated to reflux under nitrogen atmosphere with stirring for 72 h. After cooling to room temperature, CH_2Cl_2 was added and the mixture was washed three times with water. The organic phase was dried with anhydrous Na_2SO_4 and the solvent was removed by evaporation. The residues were purified by column chromatography with ethyl acetate/petroleum ether (1:10, *v*/*v*) to afford compound **3** as a light yellow solid (4.42 g, 58%). m.p. 108–109 °C (lit. 107.5–108.5 °C [35]). ^{1}H NMR (400 MHz, $CDCl_3$, ppm): δ 7.17–6.82 (m, 13H), 3.80 (s, 6H).

*4-Bis(4-methoxyphenyl)aminobenzaldehyde (**4**)*

To a solution of bis(4-methoxyphenyl)phenylamine (3.05 g, 10 mmol) and DMF (3 mL) in 1,2-dichloroethane (50 mL), $POCl_3$ (1.5 mL, 15 mmol) was added dropwise at 0 °C . Then the mixture was stirred at 70 °C for 4 h. The mixture was neutralized with a dilute aqueous solution of sodium hydroxide and extracted three times with CH_2Cl_2. The organic phase was dried with anhydrous Na_2SO_4 and the solvent was removed by evaporation. The residues were purified by column chromatography with ethyl acetate/petroleum ether (1:5, *v*/*v*) to afford the compound **4** as a yellow solid (2.46 g, 74%). ^{1}H NMR (400 MHz, $CDCl_3$, ppm): δ 9.75 (s, 1H), 7.63–7.61 (m, 2H), 7.14–7.11 (m, 4H), 6.91–6.83 (m, 6H), 3.82 (s, 6H).

*2-Amino-6-bromobenzothiazole (**6**)*

A mixture of 4-bromoaniline (10.32 g, 60.00 mmol), KSCN (58.20 g, 0.60 mol) and $CuSO_4$ (48.00 g, 0.30 mol) was stirred in methanol (80 mL) for 9 h at 70 °C. After cooling to room temperature, the suspension was filtered and the filtrate was diluted with boiling water. Ethanol was added to the boiling mixture until a clear yellow solution resulted. Cooling the solution resulted in crystallization of compound **6** as a white solid (6.46 g, 47%). m.p. 217–218 °C (lit. 215–217 °C [36]). ^{1}H NMR (400 MHz, $CDCl_3$, ppm): δ 7.71 (m, 1H), 7.43–7.38 (m, 2H), 5.25 (s, 2H).

*2-Amino-5-bromobenzenethiol (**7**)*

A mixture of 2-amino-6-bromobenzothiazole (4.58 g, 19.99 mmol) and KOH (40 g of 85% KOH in 40 mL of water) was refluxed in ethylene glycol (5 mL) under nitrogen for 48 h. After cooling to room temperature, the mixture was neutralized with acetic acid and extracted with ethyl acetate. The organic phase was dried with anhydrous Na_2SO_4 and the solvent was removed by evaporation to give the crude product (3.22 g, 79%), which was directly used for the next step.

*4-(6-Bromobenzothiazol-2-yl)-N,N-bis(4-methoxyphenyl)aniline (**8**)*

A mixture of compound **4** (2.33 g, 7.00 mmol) and compound **7** (2.86 g, 14.01 mmol) in DMSO was heated to 160 °C for 1 h. After cooling to room temperature, the mixture was poured into ice water and the precipitate was collected. The precipitate was purified by column chromatography with ethyl acetate/petroleum ether (1:20, *v*/*v*) to afford the compound **8** as a pale yellow solid (1.86 g, 53%). m.p. 162–163 °C. ^{1}H NMR (400 MHz, $CDCl_3$, ppm): δ 7.98 (m, 1H), 7.86–7.84 (m, 3H), 7.55 (m, 1H), 7.15–7.13 (m, 4H), 6.96–6.93 (m, 2H), 6.91–6.89 (m, 4H), 3.84 (s, 6H). ^{13}C NMR ($CDCl_3$, 100 MHz, ppm): δ 168.66, 156.76, 153.27, 151.51, 139.63, 136.37, 129.54, 128.55, 127.53, 124.11, 123.95, 123.59, 118.50, 117.81, 114.94, 55.51. ESI MS: *m*/*z* 518.1. Found: 519.0 $[M + H]^+$. Anal. Calcd. for $C_{27}H_{21}BrN_2O_2S$: C, 62.67; H, 4.09; N, 5.41; S, 6.20%. Found: C, 62.72; H, 4.12; N, 5.39; S, 6.23%.

*4-(2-{4-[Bis(4-methoxyphenyl)amino]phenyl}benzothiazol-6-yl)benzaldehyde (**9a**)*

Tetrakis(triphenylphosphine)palladium (84.80 mg, 0.08 mmol) was added to a mixture of compound **8** (517 mg, 1.00 mmol), 4-formylphenylboronic acid (225.00 mg, 1.50 mmol), toluene (15 mL), ethanol (10 mL) and a 2 M aqueous potassium carbonate solution (1.50 mL) under

stirring. The suspension was heated at 85 °C for 24 h under argon atmosphere. After cooling to room temperature, CH_2Cl_2 was added and the mixture was washed with water three times. The organic phase was dried with anhydrous Na_2SO_4 and the solvent was removed by evaporation. The crude product was purified with a mixture of ethyl acetate/petroleum ether (1:5, *v*/*v*) by silica column chromatography to afford the compound **9a** as a yellow solid (396 mg, 73%). m.p. 167–168 °C. ^{1}H NMR (400 MHz, $CDCl_3$, ppm): δ 10.05 (s, 1H), 8.08 (d, J = 1.6 Hz, 1H), 8.05 (d, J = 8.4 Hz, 1H), 7.96 (m, 2H), 7.87 (m, 2H), 7.80 (m, 2H), 7.70 (dd, J = 2.0, 8.4 Hz, 1H), 7.14–7.11 (m, 4H), 7.70–6.92 (m, 2H), 6.90–6.86 (m, 4H), 3.82 (s, 6H). ^{13}C NMR ($CDCl_3$, 100 MHz, ppm): δ 189.86, 169.23, 156.76, 154.50, 151.50, 146.70, 139.65, 136.14, 135.69, 135.17, 100.37, 128.61, 127.78, 127.53, 125.79, 124.39, 122.83, 120.15, 118.51, 114.95, 55.51. ESI MS: *m/z* 542.2. Found: 544.3 [M + 2]$^+$. Anal. Calcd. for $C_{34}H_{26}N_2O_3S$: C, 75.25; H, 4.83; N, 5.16; S, 5.91%. Found: C, 75.30; H, 4.85; N, 5.14; S, 5.93%.

*5-(2-{4-[Bis(4-methoxyphenyl)amino]phenyl}benzothiazol-6-yl)thiophene-2-carbaldehyde (**9b**)*

Compound **9b** was synthesized according to the procedure described for **9a**, giving a yellow solid in 44% yield. m.p. 160–161 °C. ^{1}H NMR (400 MHz, $CDCl_3$, ppm): δ 9.88 (s, 1H), 8.11 (s, 1H), 7.98 (d, J = 8.4 Hz, 1H), 7.86–7.81 (m, 2H), 7.74–7.72 (m, 2H), 7.43 (d, J = 4 Hz, 1H), 7.13–7.11 (m, 4H), 6.93–6.91 (m, 2H), 6.89–6.87 (m, 4H), 3.82 (s, 6H). ^{13}C NMR ($CDCl_3$, 100 MHz, ppm): δ 182.72, 169.726, 156.81, 155.08, 153.94, 151.63, 142.42, 139.56, 137.57, 135.80, 129.46, 128.66, 127.56, 124.89, 124.23, 124.15, 122.92, 119.21, 118.41, 114.95, 55.52. ESI MS: *m/z* 548.1. Found: 549.5 [M + H]$^+$. Anal. Calcd. for $C_{32}H_{24}N_2O_3S_2$: C, 70.05; H, 4.41; N, 5.11; S, 11.69%. Found: 70.16; H, 4.39; N, 5.13; S, 11.67%.

*5-(2-{4-[Bis(4-methoxyphenyl)amino]phenyl}benzothiazol-6-yl)furan-2-carbaldehyde (**9c**)*

Compound **9c** was synthesized according to the procedure described for **9a**, giving a yellow solid in 74% yield. m.p. 164–165 °C. ^{1}H NMR (400 MHz, $CDCl_3$, ppm): δ 9.65 (s, 1H), 8.33 (s, 1H), 8.00 (d, J = 8 Hz, 1H), 7.86–7.81(m, 4H), 7.33–7.32 (d, J = 1.6 Hz, 1H), 7.13–7.11 (m, 4H), 6.93–6.91 (m, 2H), 6.89–6.87 (m, 4H), 3.82 (s, 6H). ^{13}C NMR ($CDCl_3$, 100 MHz, ppm): δ 177.06, 169.94, 159.17, 156.82, 155.20, 152.09, 151.63, 139.60, 135.61, 128.66, 127.55, 125.23, 124.21, 123.70, 122.79, 118.42, 118.36, 114.96, 107.82, 55.51. ESI MS: *m/z* 532.2. Found: 533.6 [M + H]$^+$. Anal. Calcd. for $C_{32}H_{24}N_2O_4S$: C, 70.05; H, 4.41; N, 5.11; S, 11.69%. Found: C, 70.21; H, 4.37; N, 5.13; S, 11.67%.

*3-(4-(2-{4-[Bis(4-methoxyphenyl)amino]phenyl}benzothiazol-6-yl)phenyl)-2-cyanoacrylic acid (**Z1**)*

To a solution of **9a** (271 mg, 0.50 mmol) and 2-cyanoacetic acid (425 mg, 5 mmol) in chloroform (20 mL) was added piperidine (0.10 mL, 1 mmol). The mixture was refluxed under nitrogen for 5 h. After cooling to room temperature, the mixture was neutralized with 2 M aqueous HCl, and extracted with CH_2Cl_2 three times. The organic phase was dried with anhydrous Na_2SO_4 and the solvent was removed by evaporation. The residue was purified by column chromatography with CH_3OH/ CH_2Cl_2 (1:15, *v*/*v*) to afford the compound **Z1** as an orange solid (235 mg, 77%). m.p. 176–177 °C. ^{1}H NMR (400 MHz, DMSO-d_6, ppm): δ 8.44 (s, 1H), 8.35 (s, 1H), 8.13 (m, 2H), 8.01 (d, J = 8.4 Hz, 1H), 7.95 (m, 2H), 7.86–7.85 (m, 3H), 7.14–7.12 (m, 4H), 6.97–6.95 (m, 2H), 6.77–6.76 (m, 4H), 3.76 (s, 6H). ^{13}C NMR (DMSO-d_6, 100 MHz, ppm): δ 168.33, 163.32, 156.69, 153.95, 153.51, 151.26, 143.75, 138.72, 135.12, 135.01, 131.39, 130.47, 128.48, 127.85, 127.37, 125.54, 123.16, 122.42, 120.44, 117.03, 116.29, 115.15, 103.22, 55.26. ESI MS: *m/z* 609.2. Found: 611.1 [M + 2]$^+$. Anal. Calcd. for $C_{37}H_{27}N_3O_4S$: C, 72.89; H, 4.46; N, 6.89; S, 5.26%. Found: C, 72.84; H, 4.51; N, 6.87; S, 5.30%.

*3-(5-(2-{4-[Bis(4-methoxyphenyl)amino]phenyl}benzothiazol-6-yl)thiophen-2-yl)-2-cyanoacrylic acid (**Z2**)*

Compound **Z2** was synthesized according to the procedure described for **Z1**, giving a dark red solid in 75% yield. m.p. 172–173 °C. ^{1}H NMR (400 MHz, DMSO-d_6, ppm): δ 8.47–8.35 (m, 2H), 8.00–7.88 (m, 2H), 7.82–7.80 (m, 3H), 7.79 –7.72 (m, 1H), 7.13–7.11 (m, 4H), 6.70–6.95 (m, 4H), 6.75–6.73 (m, 2H), 3.76 (s, 6H). ^{13}C NMR (DMSO-d_6, 100 MHz, ppm): δ 168.85, 166.70, 154.36, 151.62, 151.28, 145.44, 140.40, 138.65, 135.31, 134.88, 128.79, 128.48, 127.85, 125.03, 124.66, 122.97, 122.58, 119.48, 116.90, 115.14, 55.26. ESI MS: *m/z* 615.1. Found: 616.5 [M + H]$^+$. Anal. Calcd. for $C_{35}H_{25}N_3O_4S_2$: C, 68.27; H, 4.09; N, 6.82; S, 10.42%. Found: C, 68.32; H, 3.98; N, 6.84; S, 10.45%.

*3-(5-(2-{4-[Bis(4-methoxyphenyl)amino]phenyl}benzothiazol-6-yl)furan-2-yl)-2-cyanoacrylic acid (**Z3**)*

Compound **Z3** was synthesized according to the procedure described for **Z1**, giving a red solid in 73% yield. m.p. 170–171 °C. ^{1}H NMR (400 MHz, DMSO-d_6, ppm): δ 8.50 (s, 1H), 8.00–7.95 (m, 3H), 7.86–7.84 (m, 2H), 7.41–7.35 (m, 2H), 7.23–7.15 (m, 4H), 6.78–6.96 (m, 4H), 6.76–6.75 (m, 2H), 3.76 (s, 6H). ^{13}C NMR (DMSO-d_6, 100 MHz, ppm): δ 168.55, 163.84, 156.97, 156.75, 154.17, 151.36, 148.21, 138.64, 135.02, 128.55, 127.93, 125.27, 123.22, 122.91, 122.61, 117.97, 116.86, 115.17, 109.81, 55.26. ESI MS: *m/z* 599.2. Found: 600.8 [M + H]$^+$. Anal. Calcd. for $C_{35}H_{25}N_3O_5S$: C, 70.10; H, 4.20; N, 7.01; S, 5.35%. Found: C, 70.08; H, 4.15; N, 6.91; S, 5.37%.

2.3 Fabrication of DSSCs

Fluorine-doped tin oxide (FTO) coated glass plates (15

Ω/square, Nippon Sheet Glass, Japan) were cleaned in ethanol, acetone and de-ionized water using an ultrasonic bath then rinsed with water and ethanol. TiO_2 powder (20 nm, 2.0 g) was added to a mixture of ethanol (16.0 mL), acetic acid (0.4 mL), terpineol (6.0 g) and ethyl cellulose (1.0 g), and then ground for 40 min to form a slurry. After the ultrasonic processing of the slurry, a white viscous TiO_2 paste was produced. Then a TiO_2 film (18 μm in thickness) was prepared using the screen-printing technique. The TiO_2-coated FTO glass was sintered by heating at 325 °C for 5 min, 375 °C for 5 min, 450 °C for 15 min, and then 500 °C for 15 min, then soaked in 0.04 M $TiCl_4$ solution and calcined at 520 °C for 30 min again. The prepared TiO_2 electrodes were immersed into the 0.3 mM solution of the dye in CH_3OH/CH_2Cl_2 (1:4, *v*/*v*) and kept at room temperature in the dark for 16 h. For photovoltaic performance measurements, the dye-adsorbed TiO_2 electrode and Pt counter electrode were assembled in a sealed sandwich-type cell. After the injection of the electrolyte solution, which was composed of 0.60 M 1-methyl-3-propylimidazolium iodide (PMII), 0.10 M guanidinium thiocyanate, 0.03 M I_2, 0.50 M *tert*-butylpyridine in acetonitrile and valeronitrile (85:15), through the hole made on the counter electrode into the space between the sandwiched cell, the photoelectrochemical properties of the DSSCs were measured.

3 Results and discussion

3.1 Photophysical properties

The UV-vis absorption and emission spectra of the dyes **Z1–Z3** in CH_2Cl_2 are shown in Figure 1, and the corresponding data are summarized in Table 1. All the dyes show two major absorption bands at 300–390 nm and 400–600 nm. The absorption band at 300–390 nm can be ascribed to localized aromatic π-π* transitions. The absorption band at 400–600 nm can be attributed to the intramolecular charge (ICT) transitions. The absorption maximum wavelength (λ_{max}) of **Z1–Z3** was at 425, 460, and 463 nm, and the corresponding maximum extinction coefficient was 3.64×10^4, 4.21×10^4 and 3.17×10^4 M^{-1} cm^{-1}, respectively (i.e., increasing in the order **Z3** < **Z1** < **Z2**). These maximum extinction coefficients are much higher than that of the ruthenium dye N719 (1.4×10^4 M^{-1} cm^{-1}) [2]. The λ_{max} of **Z3** with the furan linker was red-shifted 3 nm compared to that of **Z2** with the thiophene linker, while the λ_{max} of **Z2** was red-shifted 38 nm compared to that of dye **Z1** with the benzene linker. This is due to the better delocalization of electrons over the π-conjugated molecules when furan was used as linker in this D-A-π-A framework. Surprisingly, the absorption λ_{max} of **Z1–Z3** were all blue-shifted almost 40 nm after the introduction of benzothiazol in comparison with the reference dye C1 without benzothiazol [37]. When the

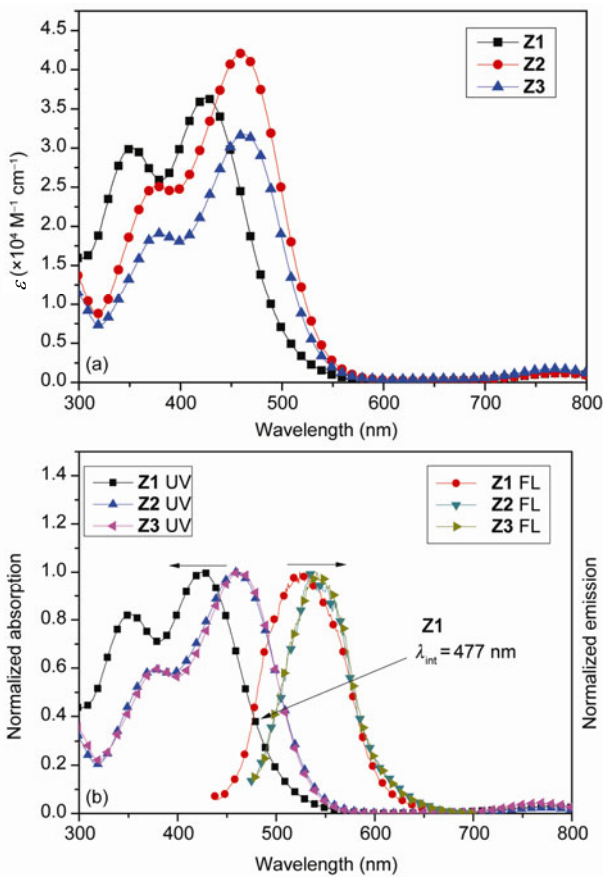

Figure 1 (a) Absorption spectra of the dyes in CH_2Cl_2; (b) normalized absorption and emission spectra of the dyes in CH_2Cl_2.

Table 1 Absorption, emission and electrochemical properties of the dyes **Z1–Z3**

Dye	Absorption			Emission	Oxidation potential data				
	λ_{max} a) (nm)	ε (×10⁴ M^{-1} cm^{-1})	λ_{max} b) (nm)	λ_{max} (nm)	E_{ox} c) (vs. NHE)	$E_{0\text{-}0}$ d) (V)	$E_{ox} - E_{0\text{-}0}$ (V, vs. NHE)	E_{gap} e) (V, vs. NHE)	E_{HOMO}/E_{LUMO} (eV)
Z1	352 425	3.00 3.64	417	527	1.43	2.60	−1.17	0.67	−5.68/−3.08
Z2	377 460	2.61 4.21	419	539	1.47	2.50	−1.03	0.53	−5.72/−3.22
Z3	379 463	1.91 3.17	419	546	1.47	2.50	−1.03	0.53	−5.72/−3.22

a) Absorption and emission spectra of the dyes in CH_2Cl_2; b) absorption spectra of the dyes anchored on TiO_2 films; c) E_{ox} measured in CH_3CN with 0.1 M $TBAPF_6$ (vs. NHE); d) $E_{0\text{-}0}$ was determined from the intersection of absorption and emission spectra in CH_2Cl_2; e) E_{gap} is the energy gap between the E_{ox} – $E_{0\text{-}0}$ of the dye and the conductive band level of TiO_2 (–0.5 V vs. NHE).

three dyes were adsorbed onto TiO_2 films (Table 1), the absorption bands of **Z1–Z3** were blue-shifted by 8, 41 and 44 nm, respectively, compared with the solution spectra. This can be explained by the formation of H-aggregates of the dye and the deprotonation of the carboxylic acid moiety upon adsorption on the film of TiO_2 [38, 39].

3.2 Electrochemical properties

To evaluate the possibility of dye regeneration and electron transfer from the excited state to the conduction band (CB) of TiO_2, cyclic voltammetry was performed to measure the first oxidation potentials (E_{ox}) corresponding to the HOMO level of the dyes. The HOMO and LUMO levels of the dyes are listed in Table 1. The schematic energy levels of **Z1–Z3** based on electrochemical data are shown in Figure 2. The first half-wave potentials of **Z1–Z3** were 0.80, 0.84 and 0.84 V. Therefore, the first oxidation potentials (E_{ox}) corresponding to the HOMO levels were 1.43, 1.47 and 1.47 V (by addition of 0.63 V to the potential vs. Fc/Fc^+ (vs. NHE)), respectively. The estimated excited state potentials corresponding to the LUMO levels were −1.17, −1.03 and −1.03 V calculated from E_{ox}–$E_{0\text{-}0}$, where $E_{0\text{-}0}$ values were calculated from the intersection (λ_{int}) of the normalized absorption and the emission spectra ($E_{0\text{-}0} = 1240/\lambda_{int}$, Figure 1(b)). The HOMO energy levels were calculated by the equation $E_{HOMO} = -e[4.88 + E_{1/2}$ (vs. Fc/Fc^+)] [40] and the E_{LUMO} levels were calculated based on the relationship $E_{LUMO} = E_{HOMO} + E_{0\text{-}0}$. The E_{HOMO} and E_{LUMO} data are summarized in Table 1. All the HOMO levels of dyes **Z1–Z3** (1.43, 1.47 and 1.47 V, Figure 2) were more positive than that of the iodine/iodide redox potential value (0.4 V vs. NHE) [41], ensuring the thermodynamic regeneration of the dyes. However, the E_{ox} of the dyes are slightly too positive, which might lower the open-circuit voltage (V_{oc}) [42]. The LUMO levels of the three dyes were more negative than the energy level of the TiO_2 electrode (−0.5 V vs. NHE) [41], allowing excited electrons to be efficiently injected into the electrode conduction band of TiO_2.

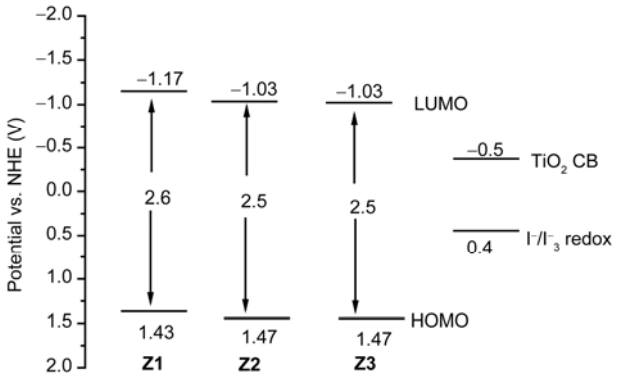

Figure 2 The schematic energy levels of **Z1–Z3** based on absorption and electrochemical data.

3.3 Theoretical calculations

The density functional theory (DFT) calculations for **Z1–Z3** were carried out using the Gaussian 09 program at the B3LYP/6–31 + G (d) levels. The electron distributions of HOMO and LUMO levels of the dyes are shown in Figure 3. It can be clearly seen that the electron density is uniformly distributed along the D-A system (triphenylamine and benzothiazole units) in the ground state; while at the LUMO level, electrons move by an intramolecular charge transfer, and are finally delocalized across the entire A-π-A system (benzothiazole-π-cyanoacrylic acid). The results indicate that the electrons can be successively transferred from the donor to the benzothiazole unit, then transferred to the cyanoacetic acid unit, and finally to TiO_2.

3.4 Photovoltaic performance

The photocurrent density-photovoltage (*J-V*) curves of the DSSCs based on **Z1–Z3** are shown in Figure 4, and key parameters including short-circuit current density (J_{sc}), open-circuit voltage (V_{oc}), fill factor (*FF*) and overall power conversion efficiency (η) are summarized in Table 2. For the three dyes, the **Z2**-sensitized cell exhibited a maximum η of 4.16% (J_{sc} = 9.27 mA cm^{-2}, V_{oc} = 642 mV, *FF*= 0.70).

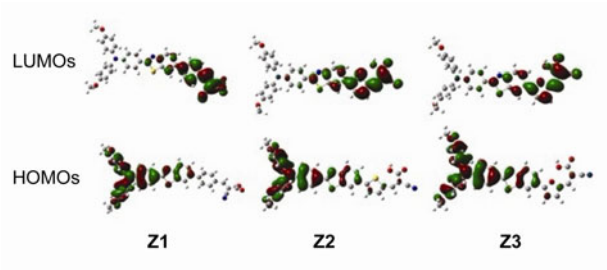

Figure 3 The optimized structure and the frontier molecular orbitals of the HOMOs and LUMOs of the dyes calculated by DFT at the B3LYP/6–31 + G (d) level.

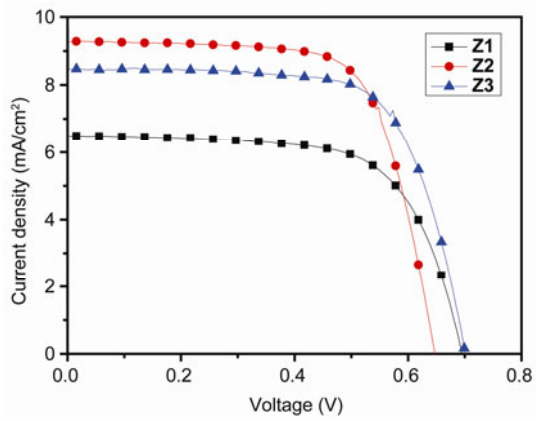

Figure 4 The current density-voltage curves of the DSSCs based on dyes **Z1–Z3** measured under the illumination of AM 1.5 G (100 mW cm^{-2}).

Table 2 Photovoltaic parameters of DSSCs

Dye	J_{sc} (mA cm^{-2})	V_{oc} (mV)	*FF*	η (%)	Adsorbed amount (×10^{-7} mol cm^{-2})
Z1	6.83	690	0.67	3.15	2.6
Z2	9.27	642	0.70	4.16	3.3
Z2 a)	9.97	671	0.69	4.61	–
Z3	8.46	695	0.70	4.12	3.8

a) Dye bath: 0.3 mM **Z2** and 3.0 mM CDCA in CH_3OH/CH_2Cl_2 (1:4, *v*/*v*).

Under the same conditions, the cells sensitized with **Z1** and **Z3** gave J_{sc} of 6.83 and 8.46 mA cm^{-2}, V_{oc} of 690 and 695 mV and *FF* of 0.67 and 0.70, corresponding to η of 3.15% and 4.12%, respectively. The **Z2**-sensitized cell has the highest η due to its relatively higher J_{sc}, which can be attributed to its broader absorption and enhanced molar extinction coefficient in the visible region. The amounts of dye adsorbed on the TiO_2 substrate increased in the order **Z1** < **Z2** < **Z3**. Although the absorbed amount of **Z2** is smaller than that of **Z3**, **Z2** has the higher J_{sc} due to its broader spectral response range.

The efficiencies of the DSSCs based on **Z1–Z3** were not as high as expected. We consider that the low efficiency is due to their relatively low ability to absorb sunlight throughout the full spectrum. In comparison with the reference dye C1 without benzothiazol [37], the absorption λ_{max} of **Z1–Z3** are blue-shifted almost 40 nm, which reduces the absorption range of sunlight, leading to the decrease of short-circuit current density (J_{sc}) and finally resulting in low efficiency of the solar cells. Normally the introduction of a benzothiazol unit extends conjugation of the dye, leading to red-shift of its light absorption. The absorption λ_{max} of **Z1–Z3** are blue-shifted because the benzothiazole unit does not conjugate well with the other units in the molecule. Thus, structural modification of these dyes to increase the conjugation of benzothiazole with the other units might improve the DSSC performance.

We studied the performance of the DSSCs based on **Z2** in the presence of chenodeoxycholic acid (CDCA) (3.0 mM in CH_3OH/CH_2Cl_2 (1:4, *v*/*v*). The results are collected in Table 2. CDCA improved the device performance, with the power conversion efficiency of the DSSC reaching 4.61%. A possible explanation is that CDCA reduced the aggregation of dye **Z2** on the TiO_2 surface [43].

The incident monochromatic photon-to-current conversion efficiency (IPCE) spectra for the DSSCs based on dyes **Z1–Z3** are shown in Figure 5. The IPCE onsets for **Z1–Z3** were extended to 600, 680 and 650 nm, respectively, increasing in the order **Z1** < **Z3** < **Z2**. The solar cells based on the **Z1–Z3** dyes exhibited IPCE values above 60% in the range 400–500 nm, with a maximum value of 79.3% at 430 nm for **Z1**, 79.9% at 470 nm for **Z2** and 75.7% at 430 nm for **Z3**, respectively. The higher IPCE value of dye **Z2** containing the thiophene moiety can be attributed to its higher light harvesting efficiency in the visible region, which matched well with its broader absorption and enhanced molar extinction coefficient in solution. The higher IPCE and J_{sc} could lead to an improved photovoltaic performance of the DSSCs based on dye **Z2**.

Among the three dyes, DSSCs based on **Z2** produced the highest J_{sc} but the lowest V_{oc}, which can be explained by the electron lifetime in the conduction band of TiO_2. Electrochemical impedance spectroscopy (EIS) was performed to investigate interfacial charge transfer in DSSCs under the dark. As is shown in Figure 6, Nyquist plots typically have three semicircles, and the large semicircle at intermediate frequencies is attributed to charge transfer resistances at the TiO_2/dye/electrolyte interface. The radius of the larger semicircle increases in the order **Z2** < **Z3** < **Z1**, implying the same order of the electron recombination resistance for the three dyes. The data of recombination resistance and

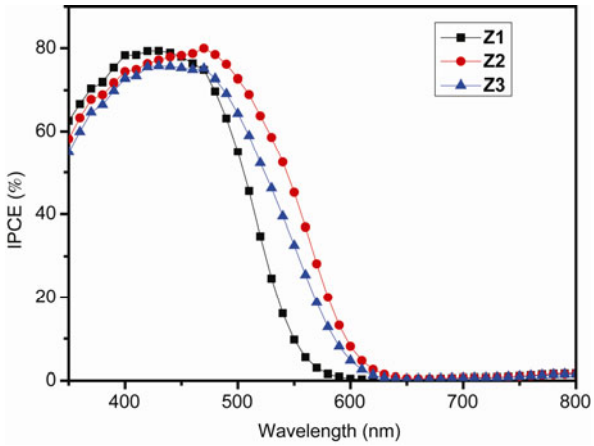

Figure 5 IPCE spectra of DSSCs based on **Z1–Z3**.

Table 3 Electrochemical parameters of DSSCs obtained from EIS

Dye	*R* (ohm)	*C* (μF)	Electron lifetime (ms)
Z1	134.1	480	64
Z2	49.4	477	24
Z3	103.3	797	82

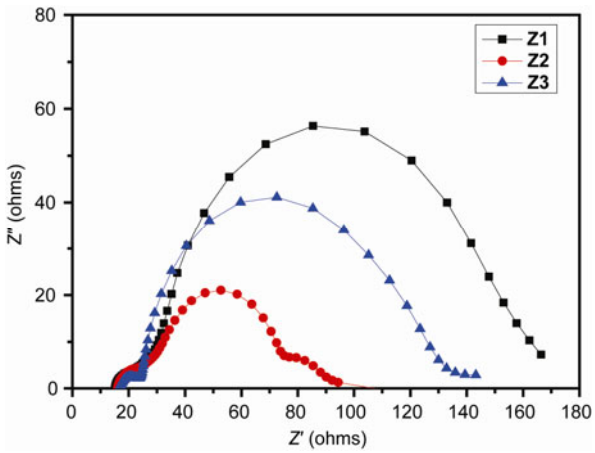

Figure 6 Electrochemical impedance spectra of the DSSCs based on **Z1–Z3** measured in the dark.

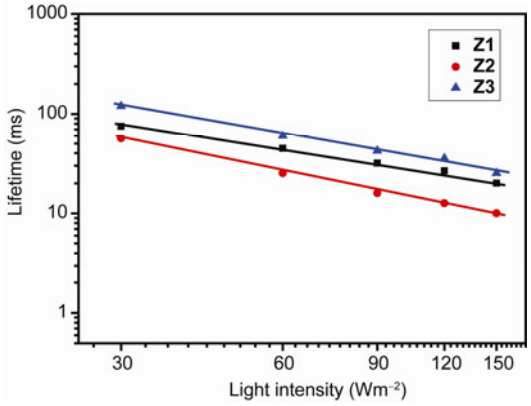

Figure 7 IMVS spectra of the DSSCs based **Z1–Z3** dyes measured under various incident light intensities.

chemical capacitance are listed in Table 3. The electron lifetime values derived from curve fittings are 64, 24 and 82 ms for **Z1**, **Z2** and **Z3** based DSSCs, respectively. The same order (**Z2** < **Z1** < **Z3**) of the electron lifetime is also shown in the IMVS (Figure 7). Although the **Z1**-based DSSCs exhibit a larger recombination resistance than **Z3**-based DSSCs, the value of the chemical capacitance of the DSSCs based on **Z3** is much larger. As a result, the electron lifetime increases in the order **Z2** < **Z1** < **Z3**. The **Z2**-based DSSCs exhibit the lowest V_{oc} (Figure 4) value due to the shortest electron lifetime among the three dye-based cells.

4 Conclusion

A series of new D-A-π-A organic dyes **Z1–Z3** containing the benzothiazole unit as an additional electron-withdrawing acceptor have been designed and synthesized. The photophysical and electrochemical properties of the D-A-π-A systems have been studied. After the introduction of a benzothiazole unit, all the three dyes showed enhanced molar extinction coefficients. The effects of various conjugated linkers (benzene, furan and thiophene) on dye-sensitized solar cell were also investigated. It was found that dye **Z2**, with a thiophene linker, gives a solar cell which exhibits the best overall light to electricity conversion efficiency η of 4.16% under standard global AM 1.5 G solar conditions. The efficiency is not high because the conjugation of the benzothiazole unit is relatively poor, leading to a decrease in the absorption range of sunlight. Further structural modifications to increase the conjugation of the benzothiazole with the other units might enhance the efficiency of such DSSCs.

This work was financially supported by the National Natural Science Foundation of China (20872038, 20873183, 21072064), and the Fund from Guangzhou Science and Technology Project, China (2012J4100003).

1 O'Regan B, Grätzel M. A low-cost, high-efficiency solar cell based on dye-sensitized colloidal TiO_2 films. *Nature*, 1991, 353: 737–740
2 Wang P, Klein C, Humphry-Baker R, Zakeeruddin SM, Gratzel M. A high molar extinction coefficient sensitizer for stable dye-sensitized solar cells. *J Am Chem Soc*, 2005, 127: 808–809
3 Islam A, Chowdhury FA, Chiba Y, Komiya R, Fuke N, Ikeda N, Nozaki K, Han LN. Synthesis and characterization of new efficient tricarboxyterpyridyl (beta-diketonato) ruthenium(II) sensitizers and their applications in dye-sensitized solar cells. *Chem Mater*, 2006, 18: 5178–5185
4 Nattestad A, Mozer AJ, Fischer MKR, Cheng YB, Mishra A, Baeuerle P, Bach U. Highly efficient photocathodes for dye-sensitized tandem solar cells. *Nat Mater*, 2010, 9: 31–35
5 Seo KD, Song HM, Lee MJ, Pastore M, Anselmi C, De Angelis F, Nazeeruddin MK, Grätzel M, Kim HK. Coumarin dyes containing low-band-gap chromophores for dye-sensitised solar cells. *Dyes Pigments*, 2011, 90: 304–310
6 Nazeeruddin MK, De Angelis F, Fantacci S, Selloni A, Viscardi G, Liska P, Ito S, Takeru B, Grätzel M. Combined experimental and DFT-TDDFT computational study of photoelectrochemical cell ruthenium sensitizers. *J Am Chem Soc*, 2005, 127: 16835–16847
7 Gao F, Wang Y, Shi D, Zhang J, Wang M, Jing X, Robin HB, Wang P, Zakeeruddin SM, Grätzel M. Enhance the optical absorptivity of nanocrystalline TiO_2 film with high molar extinction coefficient ruthenium sensitizers for high performance dye-sensitized solar cells. *J Am Chem Soc*, 2008, 130: 10720–10728
8 Grätzel M. The advent of mesoscopic injection solar cells. *Prog Photovolt: Res Appl*, 2006, 14: 429–442
9 Mishra A, Fischer MKR, Baeuerle P. Metal-free organic dyes for dye-sensitized solar cells–From structure: Property relationships to design rules. *Angew Chem Int Ed*, 2009, 48: 2474–2499
10 Hara K, Sayama K, Ohga Y, Shinpo A, Suga S, Arakawa H. A coumarin-derivative dye sensitized nanocrystalline TiO_2 solar cell having a high solar-energy conversion efficiency up to 5.6%. *Chem Commun*, 2001: 569–570
11 Hara K, Wang ZS, Sato T, Furube A, Katoh R, Sugihara H, Dan OY, Kasada C, Shinpo A, Suga S. Oligothiophene-containing coumarin dyes for efficient dye-sensitized solar cells. *J Phys Chem B*, 2005, 109: 15476–15482
12 Ono T, Yamaguchi T, Arakawa H. Study on dye-sensitized solar cell using novel infrared dye. *Sol Energy Mater Sol Cells*, 2009, 93: 831–835
13 Horiuchi T, Miura H, Sumioka K, Uchida S. High efficiency of dye-sensitized solar cells based on metal-free indoline dyes. *J Am Chem Soc*, 2004, 126: 12218–12219
14 Liu B, Zhu W, Zhang Q, Wu W, Xu M, Ning Z, Xie Y, Tian H. Conveniently synthesized isophorone dyes for high efficiency dye-sensitized solar cells: Tuning photovoltaic performance by structural modification of donor group in donor-π-acceptor system. *Chem Commun*, 2009: 1766–1768
15 Matsui M, Kotani M, Kubot Y, Funabiki K, Jin J, Yoshida T, Higashijima S, Miura H. Comparison of performance between benzoindoline and indoline dyes in zinc oxide dye-sensitized solar cell. *Dyes Pigments*, 2011, 91: 145–152
16 Wang ZS, Li FY, Huang CH. Highly efficient sensitization of nanocrystalline TiO_2 films with styryl benzothiazolium propylsulfonate. *Chem Commun*, 2000: 2063-2064
17 Chen YS, Li C, Zeng ZH, Wang WB, Wang XS, Zhang BW. Efficient electron injection due to a special adsorbing group's combination of carboxyl and hydroxyl: Dye-sensitized solar cells based on new hemicyanine dyes. *J Mater Chem*, 2005, 15: 1654–1661
18 Kitamura T, Ikeda M, Shigaki K, Inoue T, Anderson NA, Ai X, Lian T, Yangagida S. Phenyl-conjugated oligoene sensitizers for TiO_2 solar cells. *Chem Mater*, 2004, 16: 1806–1812
19 Tian HN, Yang XC, Chen RK, Zhang R, Hagfeldt A, Sunt LC. Effect of different dye baths and dye-structures on the performance of dye-sensitized solar cells based on triphenylamine dyes. *J Phys Chem C* 2008, 112: 11023–11033

20 Hagberg DP, Yum JH, Lee H, De Angelis F, Marinado T, Karlsson KM. Molecular engineering of organic sensitizers for dye-sensitized solar cell applications. *J Am Chem Soc*, 2008, 130: 6259–6266

21 Li G, Zhou YF, Cao XB, Bao P, Jiang KJ, Lin Y, Lian MY. Novel TPD-based organic D-π-A dyes for dye-sensitized solar cells. *Chem Commun*, 2009: 2201–2203

22 Im H, Kim S, Park C, Jang SH, Kim CJ, Kim K, Park NG, Kim C. High performance organic photosensitizers for dye-sensitized solar cells. *Chem Commun*, 2010, 46: 1335–1337

23 Tian Z, Huang M, Zhao B, Huang H, Feng X, Nie Y, Ping S Tan S. Low-cost dyes based on methylthiophene for high-performance dye-sensitized solar cells. *Dyes Pigments*, 2010, 87: 181–187

24 Zeng WD, Cao YM, Bai Y, Wang YH, Shi YS, Zhang M, Wang FF, Pan CY, Wang P. Efficient dye-sensitized solar cells with an organic photosensitizer featuring orderly conjugated ethylenedioxythiophene and dithienosilole blocks. *Chem Mater*, 2010, 22: 1915–1925

25 Liang M, Zong XP, Han HY, Chen C, Sun Z, Xue S. An efficient dye-sensitized solar cell based on a functionalized-triarylamine dye. *Mater Lett* 2011, 65: 1331–1333

26 Tian H, Yang X, Chen R, Pan Y, Li L, Hagfeldt A, Sun L. Phenothiazine derivatives for efficient organic dye-sensitized solar cells. *Chem Commun*, 2007: 3741–3743

27 Park SS, Won YS, Choi YC, Kim JH. Molecular design of organic dyes with double electron acceptor for dye-sensitized solar cell. *Energy & Fuels*, 2009, 23: 3732–3736

28 Tian H, Yang X, Cong J, Chen R, Teng C, Liu J, Hao Y, Wang L, Sun L. Effect of different electron donating groups on the performance of dye-sensitized solar cells. *Dyes Pigments*, 2010, 84: 62–68

29 Tsao MH, Wu TY, Wang HP, Sun IW, Su SG, Lin YC, Chang CW. An efficient metal-free sensitizer for dye-sensitized solar cells. *Mater Lett*, 2011, 65: 583–586

30 Zhu W, Wu Y, Wang S, Li W, Li X, Chen J, Wang Z. Organic D-A-π-A solar cell sensitizers with improved stability and spectral response. *Adv Funct Mater*, 2011, 21: 756–763

31 Pei K, Wu Y, Wu W, Zhang Q, Chen B, Tian H, Zhu W. Constructing organic D-A-π-A-featured sensitizers with a quinoxaline unit for high-efficiency solar cells: The effect of an auxiliary acceptor on the absorption and the energy level alignment. *Chem Eur J*, 2012, 18: 8190–8200

32 Li W, Wu Y, Zhang Q, Tian H, Zhu W. D-A-π-A featured sensitizers bearing phthalimide and benzotriazole as auxiliary acceptor: Effect on absorption and charge recombination dynamics in dye-sensitized solar cells. *ACS Appl Mater Inter*, 2012, 4: 1822–1830

33 Hrobarikova V, Hrobarik P, Gajdos P, Fitilis I, Fakis M, Persephonis P, Zahradnik P. Benzothiazole-based fluorophores of donor-π-acceptor-π-donor type displaying high two-photon absorption. *J Org Chem*, 2010, 75: 3053–3068

34 Lartia R, Allain C, Bordeau G, Schmidt F, Fiorini-Debuisschert C, Charra F, Paule M, Teulade F. Synthetic strategies to derivatizable triphenylamines displaying high two-photon absorption. *J Org Chem,* 2008, 73: 1732–1744

35 Nelson RR, Adams RN. Anodic oxidation pathways of substituted triphenylamines. II. Quantitative studies of benzidine formation. *J Am Chem Soc,* 1968, 90: 3925–3930

36 Jordan AD, Luo C, Reitz AB. Efficient conversion of substituted aryl thioureas to 2-aminobenzothiazoles using benzyltrimethylammonium tribromide. *J Org Chem,* 2003, 68: 8693–8696

37 Yu QY, Liao JY, Zhou SM, Yong S, Liu JM, Kuang DB, Su CY. Effect of hydrocarbon chain length of disubstituted triphenylamine-based organic dyes on dye-sensitized solar cells. *J Phys Chem C*, 2011, 115: 22002–22008

38 Chen R, Yang X, Tian H, Sun L. Tetrahydroquinoline dyes with different spacers for organic dye-sensitized solar cells. *J Photochem Photobiol A*, 2007, 189: 295–300

39 Lin LY, Tsai CH, Wong KT, Huang TW, Hsieh L, Liu SH, Lin HW, Wu CC, Chou SH, Chen SH, Tsai AI. Organic dyes containing coplanar diphenyl-substituted dithienosilole core for efficient dye-sensitized solar cells. *J Org Chem*, 2010, 75: 4778–4785

40 Jones BA, Facchetti A, Wasielewski MR, Marks TJ. Tuning orbital energetics in arylene diimide semiconductors. materials design for ambient stability of *n*-type charge transport. *J Am Chem Soc*, 2007, 129: 15259–15278

41 Hagfeldt A, Graetzel M. Light-induced redox reactions in nanocrystalline systems. *Chem Rev*, 1995, 95: 49-68

42 Qu SY, Hua JL, Tian H. New D-π-A dyes for efficient dye-sensitized solar cells. *Sci China Chem*, 2012, 55: 677–697

43 Chen R, Yang X, Tian H, Wang X, Hagfeldt A, Sun L. Effect of tetrahydroquinoline dyes structure on the performance of organic dye-sensitized solar cells. *Chem Mater*, 2007, 19: 4007–4015